

High- T_c -Superconductivity and Shadow State Formation in $\text{YBa}_2\text{Cu}_3\text{O}_{6+\delta}$ and $\text{Bi}_2\text{Sr}_2\text{CaCu}_2\text{O}_{8+\delta}$

S. Grabowski, J. Schmalian, and K.H. Bennemann

*Institut für Theoretische Physik, Freie Universität Berlin, Arnimallee 14,
14195 Berlin, Germany*

(August 15, 1995)

The normal and superconducting state of $\text{YBa}_2\text{Cu}_3\text{O}_{6+\delta}$ and $\text{Bi}_2\text{Sr}_2\text{CaCu}_2\text{O}_{8+\delta}$ are investigated by using the mono- and bilayer Hubbard model within the fluctuation exchange approximation and a proper description of the Fermi surface topology. The inter- and intra-layer interactions, the renormalization of the bilayer splitting and the formation of shadow bands are investigated in detail. Although the shadow states are not visible in the monolayer, we find that the additional correlations in bilayers boost the shadow state intensity and will lead to their observability. In the superconducting state we find a $d_{x^2-y^2}$ symmetry of the order parameter and demonstrate the importance of inter-plane Copper pairing.

Central questions in the theory of the high- T_c superconductors are related to the importance of the multiple CuO_2 layers within the High- T_c superconductors like $\text{Bi}_2\text{Sr}_2\text{CaCu}_2\text{O}_{8+\delta}$ (BSCCO) or $\text{YBa}_2\text{Cu}_3\text{O}_{6+\delta}$ (YBCO) and its influence on the superconducting pairing symmetry. In addition, the detailed shape of the Fermi surface (FS) is believed to be of importance for a quantitative description of transport and photoemission experiments and also for the material dependence of the transition temperature T_c [1,2]. For bilayer cuprates, neutron scattering experiments found indications that there is an antiferromagnetic coupling between nearest-neighbor layers in YBCO [3,4]. Furthermore, recent angular resolved photoemission (ARPES) experiments found evidence for two separated bands in YBCO [5,6], that might be related to the existence of two CuO_2 bands caused by a inter-plane quasi particle transfer. However, the small experimentally observed bilayer splitting in YBCO and the difficulty to resolve two CuO_2 bands in BSCCO [7,8] support the idea that the strong short ranged antiferromagnetic order in the cuprates reduces the inter-layer hopping and might be responsible for the observation of shadows of the FS [9,10] in BSCCO.

In this paper we study the bilayer Hubbard Hamiltonian within the fluctuation exchange (FLEX) approximation [11] and focus our attention in particular on YBCO and BSCCO compounds. We find that the antiferromagnetically correlated planes yield strong deformations of the quasi particle dispersions and suppression of the bilayer splitting. In addition we observe that the shadows of the FS occur only when the inter-plane coupling is considered. The superconducting state is investigated within the framework of the Eliashberg theory where the order parameter is found to have a $d_{x^2-y^2}$ symmetry with inter- and intra-layer Cooper pair formation.

Our theory is based on the general multilayer Hubbard model that will be later on specified for a bilayer system:

$$H = \sum_{i,j,l,l',\sigma} (t_{j,l'}^{i,l} - \mu \delta_{j,l'}^{i,l}) c_{i,l,\sigma}^\dagger c_{j,l',\sigma} + U \sum_{i,l} n_{i,l,\uparrow} n_{i,l,\downarrow},$$

where the hopping integrals $t_{j,l'}^{i,l}$ determine the bare dispersion $\epsilon_{\mathbf{k}}^{ll'}$ in 2D \mathbf{k} -space, i and j (l and l') are the site (layer) indices, $\delta_{j,l'}^{i,l}$ the Kronecker symbol, U the local Coulomb repulsion and μ the chemical potential. For the bilayer the interaction-free contribution of the Hamiltonian can be diagonalized with the unitary transformation \mathcal{U} yielding an antibonding ($-$) and a bonding band ($+$) with bare dispersion $\epsilon_{\mathbf{k}}^\pm$. Assuming that this symmetry holds also in the full interacting case, one can define for the normal state corresponding Greens function $G_\pm(\mathbf{k}, i\omega_m)$ with fermionic Matsubara frequencies $\omega_m = (2m+1)\pi T$ and temperature T .

In the superconducting state it is helpful to investigate the allowed symmetries of the order parameter in a multilayer system. Here we consider only singlet superconductivity and for simplicity the bilayers case although similar symmetries apply to the multilayer Hamiltonian. Note that this discussion is only related to the inter-layer effects and not restricted to a certain in plane symmetry (d - or s -wave). At first by interchanging the two electrons of the Cooper pair, it follows for the gap function in the layer representation that $\Delta_{ll'}(\mathbf{k}) = \Delta_{l'l}(-\mathbf{k})$ due to the Pauli principle. Note that the frequency indices have been omitted for clarity. In addition to the in-plane symmetries, present for a single layer, the Hamiltonian is invariant with respect to the inversion symmetry with inversion center between the layers: therefore, the gap function has a given parity $P = \pm 1$ and it follows $\Delta_{11}(\mathbf{k}) = P\Delta_{22}(-\mathbf{k})$ and $\Delta_{12}(\mathbf{k}) = P\Delta_{21}(-\mathbf{k})$. Using the in-plane symmetry $\mathbf{k} \rightarrow -\mathbf{k}$ it follows from this considerations that the gap-function for even parity pairing $P = +1$ is given in the layer representation by:

$$\Delta(\mathbf{k}) = \begin{pmatrix} \Delta_{||}(\mathbf{k}) & \Delta_{\perp}(\mathbf{k}) \\ \Delta_{\perp}(\mathbf{k}) & \Delta_{||}(\mathbf{k}) \end{pmatrix}. \quad (1)$$

Here, the gap-function can be diagonalized by the transformation \mathcal{U} of the normal state and intra-band pairing (simultaneous intra- and interlayer pairing) occurs. For

odd parity pairing $P = -1$ it follows similarly for the gap function

$$\Delta(\mathbf{k}) = \begin{pmatrix} \Delta_{||}(\mathbf{k}) & 0 \\ 0 & -\Delta_{||}(\mathbf{k}) \end{pmatrix}, \quad (2)$$

and only intra-layer pairing occurs. Hence the gap function is off diagonal in the eigenvalue representation leading to an interband pairing state. Consequently, the corresponding Eliashberg equations decouple and the symmetry with the larger T_c will determine the superconducting state. However one might argue that there will be a change from intra- to inter-band pairing or vice versa for $T < T_c$ which would be related to a second phase transition below T_c . So far this has not been observed experimentally, and we will only consider the solution with the larger energy gain of the condensate. Now, by looking at the inter-band pairing, for a given momenta two electrons from different bands that form a Cooper pair cannot origin both from the FS due the structure of the bonding and antibonding band and due to the bilayer splitting. Hence, we expect intra-band pairing to be most dominant, e.g. yielding the largest energy gain of the superconducting phase which will be treated in the following. Note that this point is also supported by weak coupling approaches as shown by Maly *et al.* [12].

Now to treat the superconducting state of the multiband Hubbard Hamiltonian we use the Nambu-Eliashberg approach where the Green's function and the off-diagonal Green's function that describes superconducting correlations are written in terms of 2×2 matrices. Here we have to account for an additional index for the layer or the eigenvalue representation [13,14]. Consequently the Eliashberg equations for intra-band pairing can be written as follows by expanding the matrix self energy in terms of Pauli matrices:

$$\begin{aligned} \Phi_{\mathbf{k},\lambda}(i\omega_n) &= \frac{T}{N} \sum_{\mathbf{k}',\lambda',n'} \frac{(\tilde{V}_{\mathbf{k}-\mathbf{k}'}^{\lambda,\lambda'}(i\omega_n - i\omega_{n'}) + U\delta_{\lambda,\lambda'})}{D_{\mathbf{k}',\lambda'}(i\omega_{n'})} \\ &\quad \times \Phi_{\mathbf{k}',\lambda'}(i\omega_{n'}), \\ X_{\mathbf{k},\lambda}(i\omega_n) &= \frac{T}{N} \sum_{\mathbf{k}',\lambda',n'} \frac{V_{\mathbf{k}-\mathbf{k}'}^{\lambda,\lambda'}(i\omega_n - i\omega_{n'})}{D_{\mathbf{k}',\lambda'}(i\omega_{n'})} \\ &\quad \times (\varepsilon_{\mathbf{k}',\lambda'} + X_{\mathbf{k}',\lambda'}(i\omega_{n'})), \\ i\omega_n(1 - Z_{\mathbf{k},\lambda}(i\omega_n)) &= \frac{T}{N} \sum_{\mathbf{k}',\lambda',n'} \frac{V_{\mathbf{k}-\mathbf{k}'}^{\lambda,\lambda'}(i\omega_n - i\omega_{n'})}{D_{\mathbf{k}',\lambda'}(i\omega_{n'})} \\ &\quad \times i\omega_{n'} Z_{\mathbf{k}',\lambda'}(i\omega_{n'}), \end{aligned}$$

where

$$\begin{aligned} D_{\mathbf{k}',\lambda'}(i\omega_{n'}) &= (i\omega_{n'} Z_{\mathbf{k}',\lambda'}(i\omega_{n'}))^2 \\ &\quad - (\varepsilon_{\mathbf{k}',\lambda'} - X_{\mathbf{k}',\lambda'}(i\omega_{n'}))^2 - \Phi_{\mathbf{k}',\lambda'}(i\omega_{n'})^2. \end{aligned}$$

Here the term $U\delta_{\lambda,\lambda'}$ accounts for the Hartree contribution which is for the diagonal elements absorbed in the chemical potential and $\varepsilon_{\mathbf{k}}^{\lambda}$ is the free dispersion that determines the FS shape. The expansion coefficients of the diagonal self energy are $i\omega_n(1 - Z_{\mathbf{k},\lambda}(i\omega_n))$ and $\chi_{\mathbf{k},\lambda}(i\omega_n)$, whereas $\phi_{\mathbf{k},\lambda}(i\omega_n) = \Delta_{\mathbf{k},\lambda}(i\omega_n)Z_{\mathbf{k},\lambda}(i\omega_n)$ is the coefficient of the off-diagonal self energy which signals superconductivity and $\Delta_{\mathbf{k},\lambda}(i\omega_n)$ is the gap function. The interactions $V_{\mathbf{q}}^{\lambda,\lambda'}$ and $\tilde{V}_{\mathbf{q}}^{\lambda,\lambda'}$ for the bilayer systems can be obtained by performing the summation of the FLEX diagrams [11] in the layer representation and are similar to the monolayer case when one considers the fact that a third dimension with two momenta points π and 0 is introduced. Furthermore for the bilayer system they have an inter-plane, $V_{\mathbf{k}}^{\perp}(i\omega_m)$, and an in-plane, $V_{\mathbf{k}}^{\parallel}(i\omega_m)$, contribution:

$$\begin{aligned} V^{++}(\mathbf{k}, i\omega_m) &= 1/2 (V_{\mathbf{k}}^{\parallel}(i\omega_n) + V_{\mathbf{k}}^{\perp}(i\omega_n)) \\ V^{+-}(\mathbf{k}, i\omega_m) &= 1/2 (V_{\mathbf{k}}^{\parallel}(i\omega_n) - V_{\mathbf{k}}^{\perp}(i\omega_n)). \end{aligned} \quad (3)$$

This set of coupled Eliashberg equations is solved self-consistently on the real frequency axis [15]. Since most photoemission experiments were performed on YBCO and in particular BSCCO systems, it is necessary for a detailed comparison of our theory with experiments to use dispersions and Fermi surfaces that are closed around the (π, π) point. Thus the FS topology is characterized by

$$\begin{aligned} \varepsilon_{\mathbf{k}}^{\pm} &= -[2t(\cos(k_x) + \cos(k_y)) + 4t' \cos(k_x) \cos(k_y) \\ &\quad + 2t''(\cos(2k_x) + \cos(2k_y)) \pm t_{\perp}] \end{aligned}$$

with intra-plane hopping integrals $t = 0.25$ eV, $t' = -0.38t$, $t'' = -0.06t$ and $t_{\perp} = 0.4t = 100$ meV [16] as explicit model for YBCO. Due to the similarity of the YBCO and BSCCO FS, we used for the later one the bare intra-plane dispersion of YBCO and $t_{\perp}(\mathbf{k}) = 1/4 t_{\perp} (\cos(k_x) - \cos(k_y))^2$ with $t_{\perp} = 0.4t$. The resulting FS is very similar to the experiments [8] and to the band structure calculations [17]. For comparison with previous results we take $U = 4t$ but notice that we find no significant changes in our data up to values of $U = 6t$.

In Fig. 1 we present our data for the effective interaction $V_{\mathbf{q}}(\omega)$ in the two dimensional Brillouin zone (BZ) for $\omega = 0$ where we have for simplicity neglected the bilayer coupling ($t_{\perp} = 0$). Note that $x = 1 - n$ is the doping concentration whereby n is the occupation number per site. Interestingly, we find commensurate peaks in the effective interaction for this compound as observed in neutron scattering experiments [3]. This results is caused by the electronic correlations since for $U = 0$ pronounced incommensurabilities are present due to the fact that $2 \mathbf{k}_{\text{FS}} \neq (\pi, \pi)$ with Fermi surface momentum \mathbf{k}_{FS} that shift the peaks in $V_{\mathbf{q}}(\omega)$ away from \mathbf{Q} . However for finite U and strong scattering rates these incommensurable structures are smeared out due to the overdamped nature of the spin excitations and a peak at \mathbf{Q}

remains. So far only the in-plane correlations in an insulated CuO_2 -plane are considered. However, when various layers are coupled like in the bilayer systems YBCO and BSCCO the influence of the inter-plane interaction $V_{\mathbf{q}}^{\perp}(\omega)$ on the superconducting state and T_c is a significant and important open question. By investigating $V_{\mathbf{q}}^{\perp}(\omega)$ for the YBCO and BSCCO parameterization with $t_{\perp} = 0.4t$ we find that the commensurabilities in $V_{\mathbf{q}}^{\parallel}(\omega)$ remain or get even more pronounced while $V_{\mathbf{q}}^{\perp}(\omega)$ has the same \mathbf{k} -dependence as $V_{\mathbf{q}}^{\parallel}(\omega)$ but with an opposite sign. This yields an antiferromagnetic correlated bilayer via the hopping t_{\perp} that is strongest for low doping concentrations, where inter- and intra-layer interactions become comparable in magnitude although we always find $V_{\mathbf{q}}^{\perp}(\omega) < V_{\mathbf{q}}^{\parallel}(\omega)$.

The formation of shadow states is an important issue in the recent research, since it concerns the transition of the quasi particle excitations with doping from the simple paramagnetic state for large x to the antiferromagnet for low x and from large FS for optimally doped systems to small FS hole pockets for low doping. Recently we discussed for a simple model dispersion with $t' = t'' = 0$ that the dynamical antiferromagnetic short range order in the cuprates leads to a transfer of spectral weight from the FS at \mathbf{k}_{FS} to its shadow at $\mathbf{k}_{FS} + \mathbf{Q}$ [18] that might lead to the observed ARPES spectra [9,10]. In this context the importance of the quasi two dimensional nature of the magnetic excitations for shadow states has been discussed recently in Ref. [19]. Now, in Fig. 2 we demonstrate the influence of the realistic YBCO or BSCCO dispersion on the shadow states for $t_{\perp} = 0$. Here we plot the spectral density $\rho_{\mathbf{k}}(\omega)$ for two doping concentrations and for \mathbf{k} near the crossing of the dispersion with the shadow of the FS near $(\pi/2, \pi/2)$ (a), for \mathbf{k} at the FS near $(\pi, 0)$ (b) and for \mathbf{k} at the shadow of the FS near $(\pi, 0)$ (c-d). Qualitatively, these data agree with our findings for the previously used model compound since we find pronounced occupied and unoccupied shadow states in the BZ as small additional satellites in the spectral density. Again, these states are not related to new quasi particles but rather to an incoherent amount of spectral weight caused by an increased scattering rate [18]. However by comparing the data for $x = 0.02$ and $x = 0.08$ as in Fig. 2 (c) and (d), we see that they become much weaker due less pronounced nesting of the FS and the corresponding much smaller magnetic interaction $V_{\mathbf{q}}(\omega)$ as can be seen in the inset and in Fig. 1. Comparing these results with the $t' = t'' = 0$ FS we find that for $x = 0.08$ the shadows are rather strong [18]. Thus the observation by Aebi *et al.* [9] can not be satisfactorily understood by considering only a single CuO_2 plane which is in agreement with the study of Ref. [22]. since the shadows were found near the optimal doping at $x \approx 0.15$.

However, as recently discussed for the $t' = t'' = 0$ model dispersion [20] the consideration of a finite t_{\perp} in-

creases the shadow state intensity due to the additional bilayer correlations. Here the fact that for low doping $V_{\mathbf{q}}^{\perp}(\omega) \approx V_{\mathbf{q}}^{\parallel}(\omega)$ lead via Eq. 3 to $V_{\mathbf{q}}^{++}(\omega) \approx 0$ and $V_{\mathbf{q}}^{+-}(\omega) \approx V_{\mathbf{q}}^{\parallel}(\omega)$ such that we find that the spectral weight is not only shifted by the momentum \mathbf{Q} , but simultaneously also from the bonding to the antibonding band and vice versa. Now by taking a finite t_{\perp} into account we find for YBCO and BSCCO-like systems that the inter-layer antiferromagnetic coupling also increases the shadow state intensity and they start to appear for $x < 0.12$ with a maximum intensity at $t_{\perp} \approx 0.4t$. Furthermore as demonstrated in Fig. 3 for YBCO we find that the most favorable region to observe shadow states in ARPES is in the neighborhood of the $(\pi/2, \pi/2)$ point, where main and shadow band are well separated. Near $(\pi, 0)$ the absolute intensity of the shadow states is largest, but they are difficult to detect because of the superposition of shadow peaks and the dominant main band contributions. Furthermore the strongest shadow band signal might not be obtained with photoemission but with an inverse photoemission measurements (IPES) as shown in Fig. 3 (a) where a pronounced shadow peak appears. However the current limited resolution of IPES measurements might impede the observability of these states. For the BSCCO system where we use a \mathbf{k} -dependent inter-layer hopping $t_{\perp}(\mathbf{k})$ as suggested by band structure calculations [17], we find similar results near $(\pi, 0)$. However on the diagonal at $(\pi/2, \pi/2)$ both bands are not splitted and the shadows of the bonding and antibonding band are at the same position.

The overall shape of the quasi particle dispersion in the bilayer compound YBCO and the shadow band formation is presented in Fig. 4 where we focus our attention on the bilayer splitting. The experimental findings concerning the bilayer splitting in the cuprates are still controversial. For YBCO Liu *et al.* [5] and Gofron *et al.* [6] found indications via ARPES for a splitting $\Delta^{exp}_{\varepsilon}(\pi, 0) = 110$ meV that is much smaller than the theoretical predictions from band structure calculations [16] whereby for BSCCO different photoemission groups come to different conclusions concerning the existence or the absence of a finite bilayer splitting [7,8]. However, from our results for the bilayer Hubbard model we conclude that the strong antiferromagnetic correlations in the high- T_c superconductors are responsible for the smallness of the bilayer splitting and might explain these interesting experimental results as also discussed by Liechtenstein *et al.* [21].

At this stage, it is of interest to compare our results with the interesting argumentation of Vilk [22] that shadow states and a variety of related phenomena appear only if the magnetic correlation length ξ is larger than the thermal de Broglie wavelength $\lambda_{th} = v_F/\pi k_B T$. Here v_F is the Fermi velocity of the system. Assuming that v_F is given by its uncorrelated value $v_F \approx \pi a t$ (a : lattice constant) would yield shadow states for low tem-

peratures only for extremely large magnetic correlation length. However, our self consistent calculations yields a self stabilization of the shadow band phenomena: the increasing quasi particle scattering rate which is related to the formation of shadow states [18] gives rise to a pronounced flattening of the correlated dispersion as can be seen in Fig. 4. This causes a renormalization and a decrease of the Fermi velocity for decreasing T . This mechanism allows observable shadow bands even for low temperatures since λ_{th} remains almost constant as a function of T and consequently $\lambda_{th} < \xi$ can be fulfilled for moderate correlation length as observed experimentally in the high- T_c superconductors. Note that the limit $T \rightarrow 0$ is still an open question although we believe that for very low temperatures the susceptibility and the correlation length ξ behave differently compared to the effective interaction in the expression for the self energy [23]. Thus this demonstrates impressively the importance of a self consistent calculation of the Fermi velocity that decreases down to $T \approx 40$ K by taking explicitly the changes of the spin fluctuation and the quasi particle spectrum into account.

In Fig. 5 we present our data for the superconducting order parameter for the YBCO model where we plot the frequency dependence of the superconducting order parameter $\phi_{\mathbf{k}}(\omega)$ at $\mathbf{k} = (\pi, 0)$ for $x = 0.08$. Here we treated the mono and bilayer Hubbard model below T_c by solving the strong coupling Eliashberg equations thereby considering the full momentum, frequency and doping dependence of the intra- and inter-layer interactions. Here one obtains one order parameter for each band, namely $\phi_{\mathbf{k}}^{\pm}(\omega)$. These are connected to the layer representation via $\phi_{\mathbf{k}}^{\pm}(\omega) = \phi_{\mathbf{k}}^{\parallel}(\omega) \pm \phi_{\mathbf{k}}^{\perp}(\omega)$, where $\phi_{\mathbf{k}}^{\parallel}(\omega)$ ($\phi_{\mathbf{k}}^{\perp}(\omega)$) describes intra- (inter-) layer Cooper pair formation. By solving these equations for the YBCO dispersion with $t_{\perp} = 0$, we find for all x a $d_{x^2-y^2}$ wave superconducting state ($T_c = 70$ K for $x = 0.08$) without the need to introduce phenomenological interactions that enforce the formation of Cooper pairs [24,25]. Note that this value is only slightly smaller than the corresponding value for $t' = t'' = 0$ ($T_c = 97$ K for $x = 0.12$) whose FS is rather similar to the $\text{La}_{2-x}\text{Sr}_x\text{CuO}_4$ (LSCO) compound. Concerning the pairing symmetry in a bilayer system also find $d_{x^2-y^2}$ pairing symmetry and similar values for the transition temperatures. Interestingly, as can be observed in Fig. 5 the d -wave state is characterized by an increasing contribution of coherent inter-layer pairing with decreasing doping, where for $x = 0.08$ Cooper pairs are formed by electrons from the same layer as from different layers with almost equal probability.

Although it is a remarkable success that spin fluctuation induced pairing interaction cause superconductivity in mono and bilayer compounds, it might be even more important to explain the rather different transition temperatures in the large family of the high- T_c super-

conductors. Here a comparison of our monolayer results for LSCO with the data of the bilayer YBCO compound shows that T_c of YBCO should be even slightly lower than for LSCO the system when all other parameters like U or the hopping t are taken to be the same which is definitely in contradiction to the experimental observations ($T_c^{\text{YBCO}} \approx 90$ K versus $T_c^{\text{LSCO}} \approx 30$ K).

However it has been recently argued that the larger T_c is YBCO is mainly due to finite size effect and to the relatively strong coupling of the unit cells [26], which is not included in our approach. This point is also supported by experiments on ultrathin YBCO layers separated by insulating $\text{PrBa}_2\text{Cu}_3\text{O}_{7-\delta}$ which show that one separated bilayer of YBCO yields $T_c \approx 20$ K and that the coupling of these bilayers boost the transition temperature to its bulk value [27,28]. In this context our findings that a single bilayer of YBCO has a smaller T_c than LSCO are in qualitative agreement with the experiment although there is still the need for a consideration of inter-bilayer effects and for understanding the importance of other ingredients of the high- T_c materials for superconductivity

In conclusion, we investigated the doping dependence of the mono- and bilayer Hubbard for the YBCO and BSCCO systems by using the FLEX approximation. The strong antiferromagnetic coupling between the layers leads to an enhanced shadow state intensity and to their observability in YBCO- and BSCCO-like models. We found that the bilayer splitting is reduced ($\sim 50\%$) and the inter-layer hopping is effectively blocked for small doping. Finally, we presented results for the superconducting which has a d -wave order parameter for mono- and bilayer compounds whereby the later one has significant inter-layer Cooper pair contributions.

-
- [1] J.H. Kim *et al.*, Phys. Rev. B **439**, 11633 (1989).
 - [2] P. Monthoux *et al.*, Phys. Rev. Lett. **67**, 3448 (1991).
 - [3] J.M. Tranquada *et al.*, Phys. Rev. B **46**, 5561 (1992).
 - [4] H.F. Fong *et al.*, Phys. Rev. Lett. **75**, 316 (1995).
 - [5] R. Liu *et al.*, Phys. Rev. B **46**, 11056 (1992).
 - [6] K. Gofron *et al.*, Phys. Rev. Lett. **73**, 3302 (1994).
 - [7] H. Ding *et al.*, Phys. Rev. Lett. **76**, 1533 (1996).
 - [8] Z.X. Shen and D.S. Dessau, *Phys. Rep.* **253**, 1 (1995).
 - [9] P. Aebi *et al.*, Phys. Rev. Lett. **72**, 2757 (1994).
 - [10] S. LaRosa *et al.*, submitted to Phys. Rev. Lett..
 - [11] N.E. Bickers *et al.*, Phys. Rev. Lett. **62**, 961 (1989).
 - [12] J. Maly *et al.*, Phys. Rev. B **53**, 6786 (1996).
 - [13] P. Monthoux and D.J. Scalapino, Phys. Rev. Lett. **72**, 1874 (1994).
 - [14] S. Grabowski, M. Langer, J. Schmalian, and K.H. Bennemann, Europhys. Lett. **34**, 219 (1996).
 - [15] J. Schmalian, M. Langer, S. Grabowski, and K.H. Bennemann, Comp. Phys. Comm. **93**, 141 (1996).

- [16] O.K. Andersen *et al.*, **56**, 1573 (1995).
- [17] S. Massidda *et al.*, Physica C **152**, 251 (1988).
- [18] M. Langer, J. Schmalian, S. Grabowski, and K.H. Bennemann, Phys. Rev. Lett. **75**, 4508 (1995).
- [19] Y.M. Vilk and A.-M.S Tremblay, Europhys. Lett. **33**, 159 (1996).
- [20] S. Grabowski, M. Langer, J. Schmalian, and K.H. Bennemann, preprint.
- [21] A.I. Lichtenstein *et al.*, preprint.
- [22] Y.M. Vilk, preprint cond-mat/9605189.
- [23] J.J. Deisz, D.W. Hess, and J.W. Serene, Phys. Rev. Lett. **76**, 1312 (1996).
- [24] T. Dahm and L. Tewordt, Physica C **246**, 61 (1995).
- [25] T. Dahm, D. Manske, and L. Tewordt, Phys. Rev. B **54**, 602 (1996).
- [26] T. Schneider *et al.*, Europhys Lett **14**, 261 (1991).
- [27] Q. Li *et al.*, Phys. Rev. Lett. **64**, 3084 (1990).
- [28] D.H. Lowndes *et al.*, Phys. Rev. Lett. **65**, 1160 (1990).

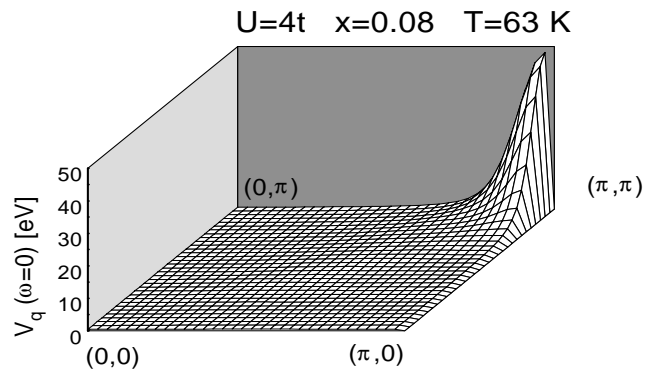


FIG. 1. Effective interaction $V_{\mathbf{q}}(\omega = 0)$ of the BSCCO/YBCO model. Note the commensurate structures, e.g. the fact that $V_{\mathbf{q}}(\omega = 0)$ is peaked at (π, π) as observed in experiments.

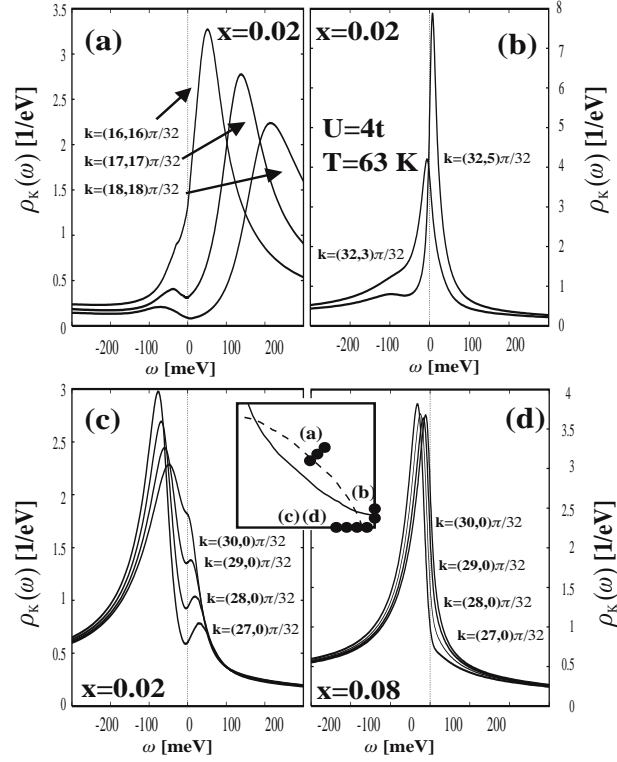


FIG. 2. Spectral density $\rho_{\mathbf{k}}(\omega)$ for the BSCCO/YBCO dispersion for \mathbf{k} points as indicated in the inset and two doping concentrations. (a): Crossing of the shadow of the Fermi surface on the diagonal in the BZ. (b): Fermi surface crossing near $(\pi, 0)$. (c) and (d): Crossing of the shadow of the Fermi surface near $(\pi, 0)$ for $x = 0.02$ and $x = 0.08$.

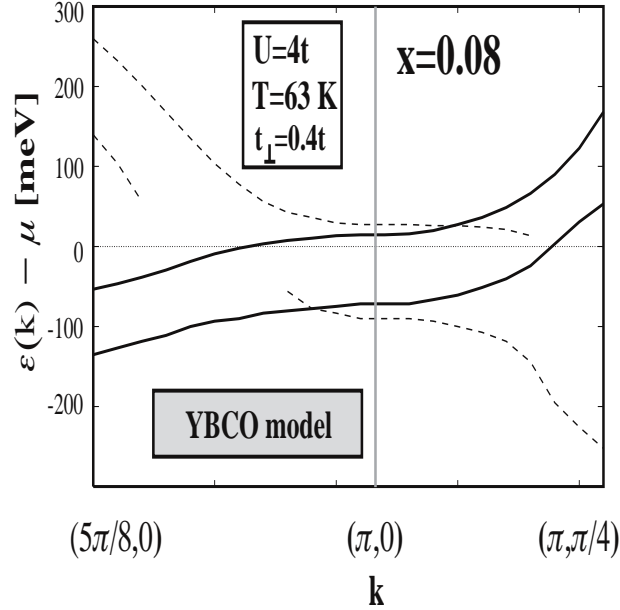


FIG. 3. Formation of shadow states for YBCO. (a): $\rho_{\mathbf{k}}^-(\omega)$ near $(\pi, 0)$. (b): $\rho_{\mathbf{k}}^-(\omega)$ on the diagonal near $(\pi/2, \pi/2)$. For simplicity only the FS of the bonding band and the shadow of the antibonding band are shown in the inset.

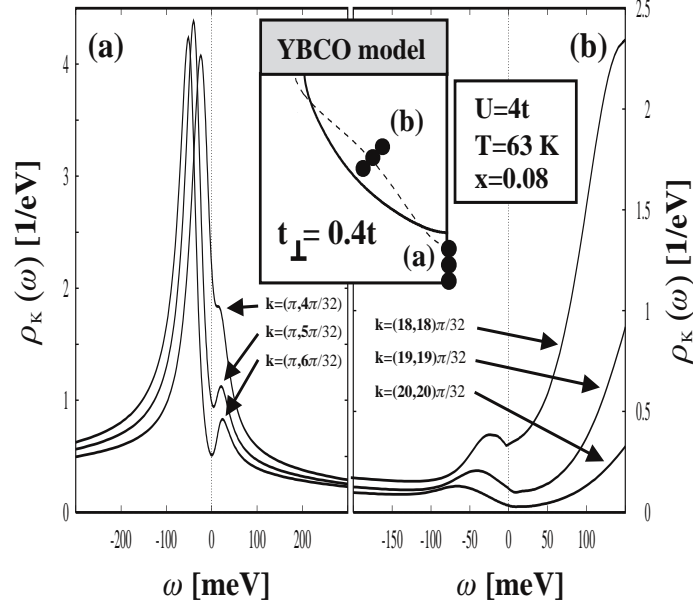


FIG. 4. Quasi particle dispersion of the bilayer BSCCO and the YBCO model (solid lines: main bands, dashed lines: shadow bands). Note the strong suppression of the bilayer splitting from $\Delta\varepsilon = 200$ meV for $U = 0$ to $\Delta\varepsilon_{(\pi,0)} = 86$ meV.

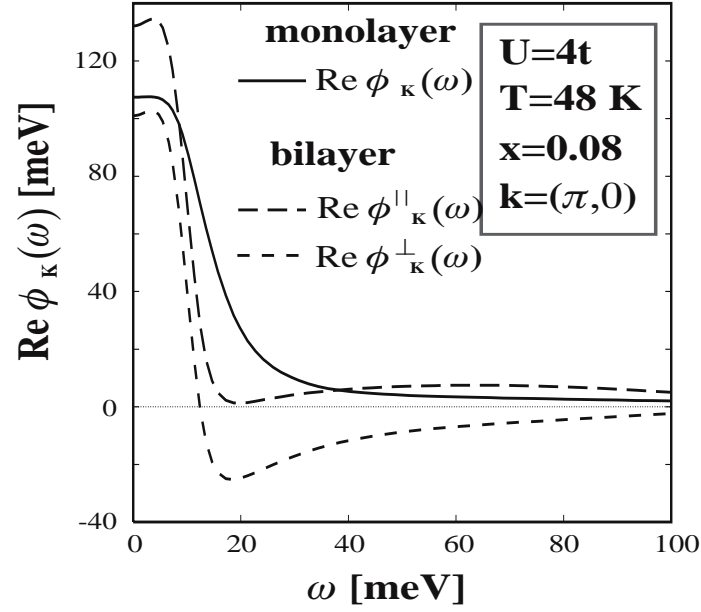


FIG. 5. Superconducting order parameter $\text{Re } \phi_{\mathbf{k}}(\omega)$ for the monolayer ($t_{\perp} = 0$) and for the bilayer with $t_{\perp} = 0.4 t$ at $\mathbf{k} = (\pi, 0)$ and the YBCO dispersion. Note the large contribution of the inter-layer Copper pair formation.